AIAA JOURNAL
Vol. 41, No. 2, February 2003

Comparisons of Initially Turbulent, Low-Velocity-Ratio Circular and Square Coaxial Jets

Dimitris E. Nikitopoulos* and Jason W. Bitting†
Louisiana State University, Baton Rouge, Louisiana 70803
and
Sivaram Gogineni‡
Innovative Scientific Solutions, Inc., Dayton, Ohio 45430

A qualitative and quantitative comparison between unforced flows emanating from equivalent geometries of axisymmetric (circular) and square coaxial nozzles is presented. The initial state of the jets is turbulent, as in nozzles relevant to practical applications. Flow visualization and velocity measurements were performed at a coflow-jet Reynolds number of 1.9×10^4 and at an inner-to-outer jet velocity ratio of 0.3. Scaling of mean velocity and turbulence profiles has been examined for the three shear layers formed in the near field of axisymmetric and square coaxial flows. Visualizations and local velocity measurements have indicated modest mixing enhancement when square nozzles are used compared to the axisymmetric ones, and this is largely attributed to differences in initial velocity profiles between these two configurations. Low-coherence, large-scale periodic structures were observed for both nozzle configurations in the midfield of the inner mixing region, which has wake characteristics. The outer mixing region, which is initially highly turbulent, shows no signs of an "indigenous" organized structure. The spectral characteristics of the circular and square nozzle combinations are qualitatively similar. However, the discrete frequency peaks associated with the wake of the inner mixing region are much broader in the case of the square nozzles. More important, the dominant frequency at the end of the midfield within the inner mixing region is lower in the case of the square nozzles compared to that of the circular ones. Spectra from the turbulent shear layers of the middle mixing region in the near field indicate the presence of a short-lived shear layer preferred mode at a much higher frequency than the one associated with the subsequent development of the wake downstream. The existence of axis switching, a phenomenon observed in single nonaxisymmetric nozzles, is not evident from visualizations and measurements in the square coaxial nozzle, presumably due to the initial low coherence of large-scale structures in the shear layers.

Nomenclature

A	=	amplitude
D	=	hydraulic diameter or length scale
f	=	frequency
Re	=	Reynolds number
U	=	mean velocity
u'	=	rms velocity fluctuation
x	=	streamwise coordinate
y	=	cross-stream coordinate
ΔU	=	mean velocity difference across the shear layer at its origin
δ	=	shear-layer thickness $\lvert y_{0.9} - y_{0.1} \rvert$
η	=	dimensionless cross-stream coordinate (shear-layer scaling)
λ	=	inner-to-outer jet average velocity ratio

Subscripts

avg	=	arithmetic average of inner and outer jet flow peak values
cl	=	centerline value
io	=	outer dimension of inner nozzle
max	=	maximum
min	=	minimum
o	=	outer jet quantity
oo	=	outer nozzle dimension
0.1	=	mean velocity is 10% of the shear-layer velocity difference
0.5	=	mean velocity is 50% of the shear-layer velocity difference
0.9	=	mean velocity is 90% of the shear-layer velocity difference

Received 1 May 2001; revision received 25 June 2002; accepted for publication 1 July 2002.

*Voorhies Associate Professor, Center for Turbine Innovation and Energy Research, Mechanical Engineering Department. Member AIAA.
†Graduate Student, Mechanical Engineering Department.
‡Senior Research Engineer. Associate Fellow AIAA.

Introduction

COAXIAL nozzles are an integral part of many engineering systems where mixing of different fluid streams is required. They are used to provide mixing between fuel and oxidizer in combustors of propulsion systems and power-producing gas-turbine systems, as well as waste combustion and incineration systems. Single noncircular nozzles have been shown to have better mixing characteristics than their axisymmetric counterparts. Therefore, combinations of such nozzles into coaxial configurations is promising. The present work aims at qualitatively and quantitatively investigating the near-field flow structure of square coaxial nozzles relative to equivalent axisymmetric coaxial jets under turbulent initial conditions, which are more typical of practical nozzles.

A good deal of work on circular coaxial nozzles has been performed as described in a series of papers. Ko and Kwan[1] provide information about the velocity and turbulence fields of coaxial jets with different inner to annular air velocity ratios λ. Subsequent work by Ko and Au[2] has examined mean flow and turbulence scaling for the same flows. A thorough flow visualization study by Dahm et al.[3] shows the large-scale vortical structures and their interactions for various λ at low Reynolds numbers. Tang and Ko[4] studied forced coaxial jets for a velocity ratio of 0.3 and showed that the initial region of the jet plays an important role in the downstream development of large-scale structures.

Regarding noncircular nozzles, several configurations have been researched to date for a single jet, including rectangular/square, triangular, lobed, and elliptic.

The rectangular and square nozzles produce noncircular vortex rings at the exit, which then deform and, under certain conditions, can lead to a switching of the jet axis. The axis switching is caused primarily by deformation and self-induction in regions of high curvature on the vortex ring produced by the sharp corners of the nozzle and depends on the initial velocity and vorticity characteristics.[5] Early studies by Sforza et al.,[6] Trentacoste and Sforza,[7] and duPlessis et al.[8] investigated square jets, but no insight was given to the underlying fundamental behavior of the square jet vortical interactions. Quinn and Militzer[9] showed that the square jet had faster spreading rates at similar distances from the exit as compared to an equivalent circular jet. A detailed numerical simulation by Grinstein et al.,[10] accompanied by an experimental investigation, illustrated that the axis switching is due to self-induction governed by the Biot–Savart law with hairpin vortices developing along the diagonals of the square jets. Their study also highlighted the effect of initial conditions and concluded that azimuthal uniformity in shear-layer momentum thickness, low small-scale turbulence levels, and a high level of shear-layer large-scale structure at the exit are favorable to the development of axis switching. Off-center velocity peaks (vena contracta effect) have been observed by Quinn[11] for a square slot orifice exit, which also favored the development of axis switching. Zaman's[5] study of rectangular jets, with and without tabs, has also provided valuable insight into the role of initial conditions and streamwise vorticity in promoting or suppressing axis switching through coupling with azimuthal vorticity dynamics.

The triangular jet has also been investigated by Schadow et al.[12] The process of self-induction in the corners of the triangle produced enhanced mixing in that region. The flow results were different for triangular orifice exits or pipe/nozzle, emphasizing the importance of initial conditions. A numerical and experimental study by Koshigoe et al.[13] explained the differences and formulated conditions for which axis switching occurs. Enhancement in the fine-scale mixing and combustion stability in the corner regions of the triangular jet were verified by Schadow et al.[14] Large-scale mixing was accomplished on the flat sides with reduced pressure oscillations as compared to the circular jet.

Elliptic jets have been studied extensively,[15–19] exhibiting axis switching and self-induction characteristics as in triangular and rectangular jets. Indeed, Husain and Hussain[16–18] have identified and described the axis-switching mechanism and its relation to azimuthal vortex dynamics, providing the basis for similar interpretations in other geometries. In terms of mixing enhancement, Gutmark and Ho[19] have documented entrainment rates in 2:1 elliptic jets that are eight times higher than a similar circular jet.

Although single noncircular nozzles have been shown to be promising in terms of improved mixing, coaxial configurations of such nozzles have hardly been studied. Bitting et al.[20] presented flow visualization results for various combinations of noncircular (square, triangular, lobed) and axisymmetric coaxial nozzles for various intermediate Reynolds numbers and low velocity ratios and made preliminary comparisons between circular and square geometries.[21] In this paper, we have studied the flow structure of a square coaxial nozzle at a single coflow Reynolds number and two inner-jet velocity ratios and have compared the results with the corresponding axisymmetric coaxial jet flows.

Experimental Setup and Methods

The test facility used for this study incorporates a modular design that allows easy exchange of inner and outer nozzles with different lip geometries. The test facility uses two independent airflow supplies. Four 25.4-mm (1-in.) lines provide air to the inner nozzle, and eight 6.35-mm ($\frac{1}{4}$-in.) lines provide air to the outer nozzle. On each main supply line, an orifice flow meter is used to determine the airflow rate. Valved, bypass ports allow the use of part of the metered air streams for seeding purposes. The inner jet flow passes through a flow-straightening honeycomb screen before entering the jet contraction with a contraction ratio of approximately 19:1. The outer jet flow reaches the outer jet through an annular passage with a contraction ratio of approximately 8:1. No attempt was made to condition the flow in either nozzle, other than the flow straightener of the inner flow, as would be the case in a practical situation. Furthermore, the flow conditions were selected so that the estimated shear-layer modes at the exit would not resonate with acoustic modes of the facility, which would be tantamount to "passive" forcing of the shear-layer, large-scale structure.

A circular coaxial nozzle with an inner diameter of 15.24 mm (0.6 in.) and an outer diameter of 38.1 mm (1.5 in.) has been used as the baseline nozzle for the square, coaxial nozzle flow study. With the preceding dimensions, the hydraulic (effective) diameter of the inner jet and outer jet is 15.24 and 19.05 mm, respectively. For the square nozzles, the hydraulic diameters are the same as for the circular jet for proper near-field comparisons between the two nozzles. The inner-to-outer-area ratio is preserved at 0.213. Note that matching the hydraulic diameters between the circular and square nozzles was deemed appropriate for the near-field comparisons of the present study. The reasoning behind this is that the flow in the near field is influenced by the conditions at the exit, which are a product of an internal flow. Thus, the hydraulic diameter is more relevant to the near field.[21] The traditional matching of nozzle flow areas is more relevant to the far field.

Visualizations have been carried out using a pulsed laser sheet and seeding with $TiCl_4$, which, on reaction with moisture produces fine submicrometer TiO_2 particles. A summary of seeding strategies that have been used to visualize selectively the shear layers in the near field of the nozzles are presented in Table 1. Instantaneous and time-averaged cuts have been made with a laser sheet from a Nd-YAG laser pulsing at 10 Hz. Visualizations on a horizontal plane (perpendicular to the jet axis) have also been carried out at various distances form the jet exit. These were achieved by a horizontal laser sheet and a mirror positioned above it at an angle of 45 deg with respect to the vertical jet axis. Thus, the top-view image was reflected horizontally into the receiving camera lens. The distance between the mirror and the exit of the jet was adequately large to avoid interference with the flow. Short (10-ns) exposures have been taken with a high-resolution Kodak charge-coupled device (CCD) array (3060 × 2036) camera, to visualize the instantaneous structure of the jets, whereas long exposures (2 s) have been used to provide a 20-realization average of the mixing regions. The resolution of the visualization images ranged from 63 μm/pixel for the side views (streamwise planes) to 33 μm/pixel for the top views (cross-stream planes).

Constant-temperature anemometry (CTA) measurements were carried out using a properly calibrated single-element probe with a spatial resolution of 2.7% of the outer hydraulic diameter (sensing length of 0.508 mm). The sensor was oriented parallel to the direction of traverse and perpendicular to the dominant direction of the airflow. The directions of the traverses used to determine velocity profiles across the jets are shown in Fig. 1. Data were collected using the TSI IFA300 system with a sampling rate of 10,000 Hz,

Table 1 Seeding strategy for visualization of the various mixing regions of the coaxial jets

Strategy no.	Visualization domain/airstream	Inner	Outer	Ambient
1	Inner and outer jet shear regions combined	H_2O (v)	$TiCl_4$	H_2O (v)
2	Outer jet shear regions only	Dry air	$TiCl_4$	H_2O (v)
3	Inner jet shear regions only	$TiCl_4$	H_2O (v)	H_2O (v)
4	Merged outer shear regions	$TiCl_4$	Dry Air	H_2O (v)

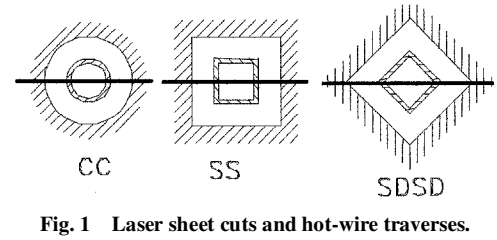

Fig. 1 Laser sheet cuts and hot-wire traverses.

low-pass filter cutoff of 5000 Hz, and sample size of 10,000 points for mean flow and turbulence intensity measurements. The velocity resolution was approximately 0.1 m/s (or 0.8% of the outer flow average velocity) with an accuracy of the same magnitude. Velocity spectra were acquired along the jet centerline and in the shear layers at the location of maximum turbulent rms fluctuation. The sample size was increased to 256,000, and the spectra were calculated for blocks of 10,000 points with 50% overlap and ensemble averaged over approximately 50 blocks.

Results and Discussion

The visualization results and local quantitative measurements to be presented here are from axisymmetric and square coaxial nozzle flows at an outer flow $Re_0 = 1.9 \times 10^4$. This Reynolds number is based on the outer nozzle hydraulic diameter and average velocity. The inner-to-outer jet average velocity ratio λ was 0.3.

Flow Visualizations

An instantaneous planar flow visualization along the center plane of the square coaxial nozzle is shown in Fig. 2. This visualization was achieved through strategy 1 (Table 1) and reveals the fine structure of the shear layers due to the initially highly turbulent and three-dimensional flowfield. Evidence of a somewhat organized large-scale structure, obscured by smaller-scale eddies, can be observed in the shear layers of the near field. Many well-defined, apparently three-dimensional, vortical structures are seen to be injected into the ambient air, which is an indication of the strongly intermittent character of the mixing process. Similar features were observed for the axisymmetric coaxial nozzle, the visualizations of which are not shown here for the sake of brevity.

In Fig. 3, instantaneous planar visualizations perpendicular to the jet axis, taken with the same seeding strategy as in Fig. 2, visually show the variation of the jet shear-layer cross sections in the near field at various distances from the jet exit. The axisymmetric (circular) jet exhibits, on average, an axisymmetric flow pattern (Figs. 3Ca and 3Cb), whereas the square jet shear layers retain the geometrical shape of their origin for several outer hydraulic diameters (Figs. 3Sa and 3Sb). However, at the farthest location from the jet exit (Fig. 3Sc), the square jet mixing regions evidently tend to loose the memory of the original shape. Intense intermittency, manifested by injections of three-dimensional vortical structures of various scales, is evident at the edges of both the inner and outer shear layers, as also seen in the axial plane visualization of the square jet in Fig. 2. The injected structures often penetrate from one mixing layer to the other, across the outer jet unmixed region, as evidenced, for example, in Figs. 3Cb, 3Sa, and 3Sb. A region of interaction between the inner and outer shear layers of the coflow is observed in the middle of the sides of the outer shear layer. This indicates strong interaction between the inner and outer shear layers in the square jet, which was not observed in the axisymmetric jet until further downstream, and this is indicative of faster merging of the outer and inner mixing regions in the case of the square nozzle geometry. The horizontal planar visualizations of Fig. 3 also show that the large-scale symmetries of the flow expected on the basis of the nozzle geometry are still present in the near field, whereas no strong evidence of azimuthal organized large-scale structures can be observed. In addition, no strong visual evidence of axis switching is present in the visualizations of the square jets in the near field.

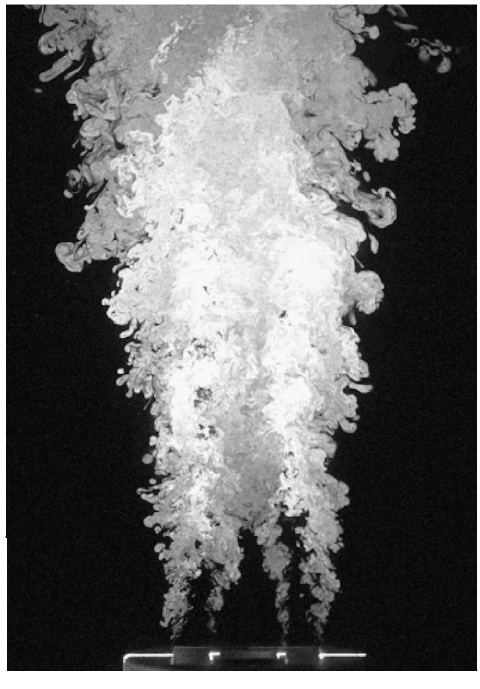

Fig. 2 Instantaneous visualization of a coaxial square jet ($Re_0 = 1.9 \times 10^4$ and $\lambda = 0.3$).

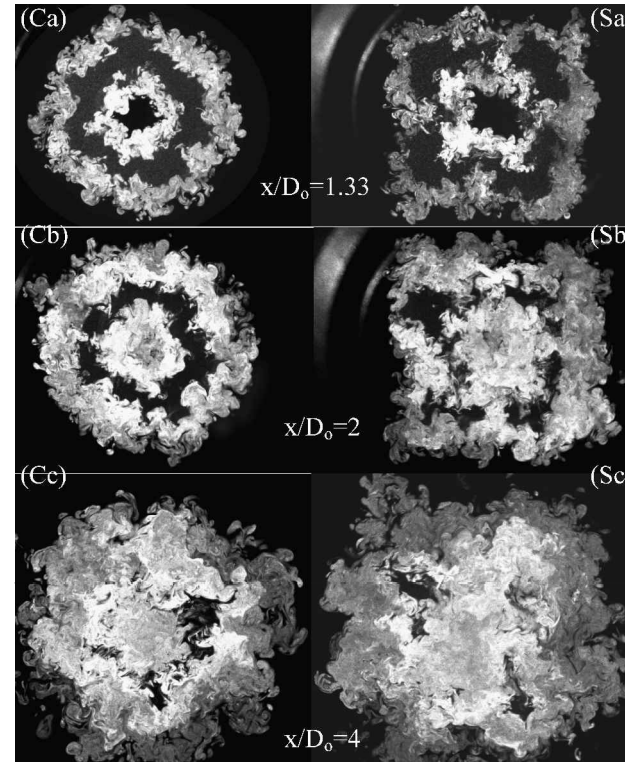

Fig. 3 Instantaneous horizontal laser sheet visualizations of equivalent circular (Ca, Cb, and Cc) and square (Sa, Sb, and Sc) coaxial jets ($Re_0 = 1.9 \times 10^4$ and $\lambda = 0.3$).

Figure 4 presents instantaneous visualizations of the outer shear layer (Figs. 4a, 4c, and 4e) and inner jet mixing region (Figs. 4b, 4d, and 4f) separately for the square (Figs. 4a and 4b on a centerplane perpendicular to the square sides and Figs. 4c and 4d on a diagonal plane) and axisymmetric (Figs. 4e and 4f on a diametral center plane) coaxial nozzles. The outer shear layer was visualized using seeding strategy 2 (Table 1) and the inner shear layer and jet was visualized using seeding strategy 3. Two planar visualization cuts are shown for the square nozzle, one perpendicular to the square side through the centerline (Figs. 4a and 4b) and one on the diagonal plane (Figs. 4c and 4d). Only half of each jet field is shown. Figures 4b, 4d, and 4f indicate that the inner jet flow is rapidly mixed with the coflow air, as seen by the brighter (heavily seeded) areas at the end of the jet unmixed core. As expected, because of the higher coflow velocity, the "outward" transport is limited as shown by the tracer pattern. The mixing boundary between the coflow and inner jet flow exhibits fine-scale, "wispy" structures that seem to be more stretched. This is also evident from the outer shear-layer visualizations of Figs. 4a, 4c, and 4e. The instantaneous realizations of the outer shear layer bear evidence of large-scale structures obscured by smaller scales, as in Fig. 2. A streamwise instability of the inner jet is also outlined by the streamwise wavering of the inner jet column. The outer shear layer appears thickest across the side of the square nozzle (Fig. 4a) and is thinner along the diagonal (Fig. 4c), as it is for the axisymmetric

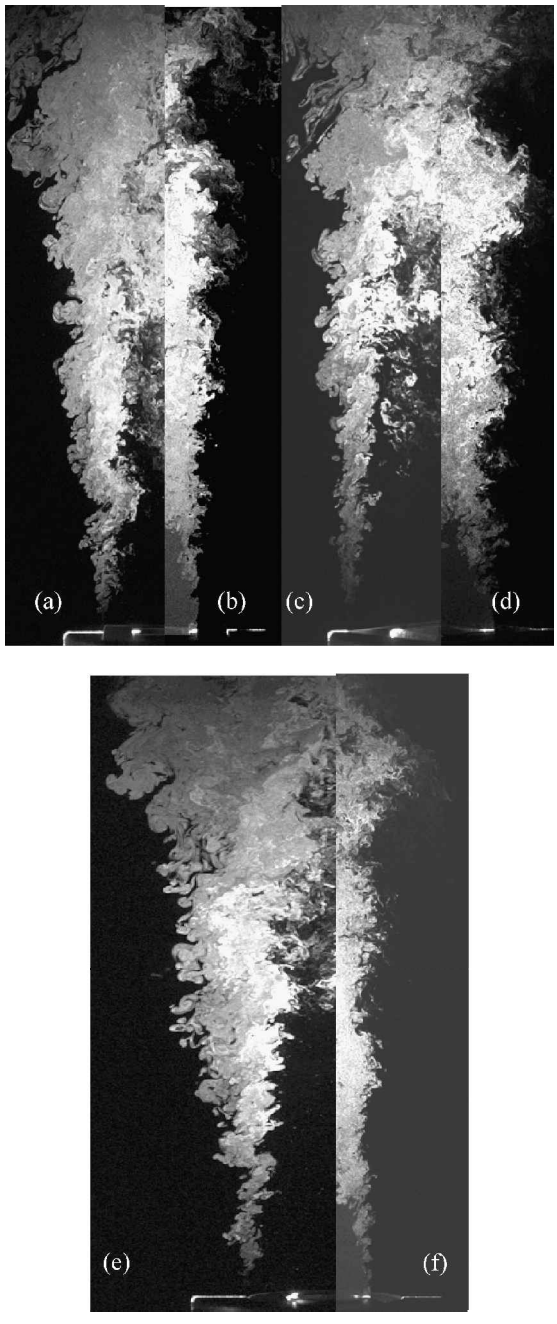

Fig. 4 Instantaneous coaxial jet flow visualizations ($Re_0 = 1.9 \times 10^4$ and $\lambda = 0.3$): a) square side, outer mixing region; b) square side, inner mixing region; c) square diagonal, outer mixing region; d) square diagonal, inner mixing region; e) axisymmetric, outer mixing region; and f) axisymmetric, inner mixing region.

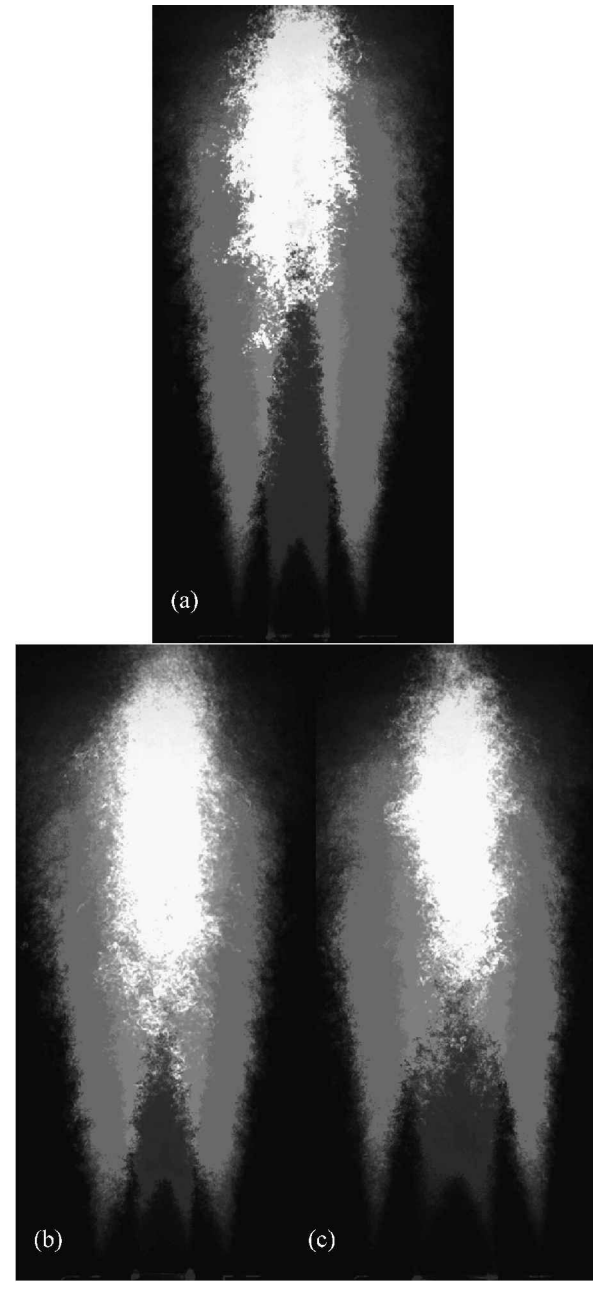

Fig. 5 Averaged visualizations of the mixing regions of a) circular coaxial nozzle flow (diametric plane-section CC in Fig. 1), b) square coaxial nozzle (center plane-section SS in Fig. 1), and c) square coaxial nozzle (diagonal plane-section SDSD in Fig. 1). $Re_0 = 1.9 \times 10^4$ and $\lambda = 0.3$.

nozzle (Fig. 4e). The intermittent presence of the tracer in the central region of the jet in Figs. 4a, 4c, and 4e, indicates that transport from the outer shear layers has started. It is evident from Figs. 4a, 4c, and 4e that such transport is somewhat delayed in the axisymmetric case compared to the square. The outer shear layer inward growth appears to be more rapid for the square nozzle in the near field.

Time-averaged visualizations of the mixing regions for the square and the corresponding circular coaxial nozzle flows are shown in Fig. 5. Each image is a gray-scale superposition of three separate time-averaged visualizations. The outer mixing region appears as gray. The inner mixing region appears as a darker shade of gray. The fully mixed region, visualized using seeding strategy 4 (Table 1) appears as white. In this last case, the reaction between $TiCl_4$ and moisture can take place to produce the visible titanium oxide seed particles only when moist ambient air penetrates the outer mixing region into the core of the jet. The overlap between the inner and outer mixing regions appears as light gray. The unmixed cores (inner and outer) and the ambient region are black.

It appears from Fig. 5 that the fully mixed region begins at an earlier location for the square nozzles compared to the circular ones. The outer unmixed cores disappear sooner for the square nozzles in the region between the parallel square sides (Fig. 5b) compared to the diagonal plane (Fig. 5c) and the circular nozzles (Fig. 5a). This indicates improved, yet localized, mixing with the square nozzles. The velocity measurements presented in the next section indicate that this improved mixing stems from higher outer-flow initial turbulence levels in the region between the parallel square-nozzle sides compared to those of the circular one.

Velocity and Turbulence Profiles

Axial mean velocity and velocity fluctuation profiles have been measured across the jets at various downstream locations from the jet origin covering the near field of the coaxial jets. Samples of these profiles are shown in Fig. 6, superimposed on time-averaged

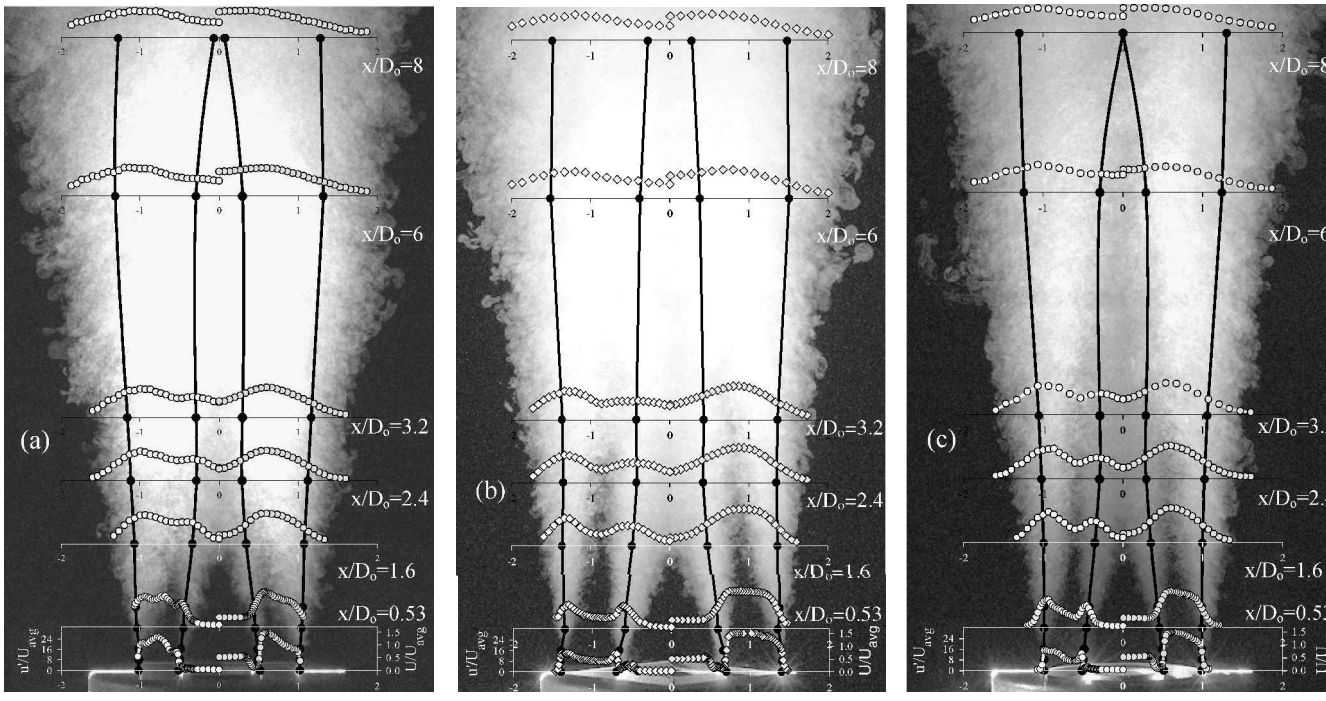

Fig. 6 Visualization and measurement of the flow evolution in coaxial nozzles at $Re_0 = 1.9 \times 10^4$ and $\lambda = 0.3$: a) square SS plane, b) square SDSD plane, and c) axisymmetric CC plane: ○, streamwise mean velocity; ⊖, streamwise velocity fluctuation; –●–, outer shear layer ($U_{max} - U_{min}$)/2 width; and –●- -, middle shear layer ($U_{max} - U_{min}$)/2 width.

visualizationsof the flow. Two sets of profiles are given for the square nozzle case; one parallel to the square jet sides along the plane of symmetry (SS in Fig. 1) and one along the diagonal (SDSD in Fig. 1), as is customary in previous single square jet investigations.[10] The velocities are scaled with the arithmetic average of the maximum velocities of the inner and coflow streams at the exit of the coaxial jets. The difference between these average velocity scales between the axisymmetric and square cases is less than 3%, and so this scaling does not produce a misleading picture. All lengths are scaled with the outer jet hydraulic diameter D_o.

The streamwise development of the shear layers existing in the near field of the axisymmetric and square coaxial jets examined appears quantitatively in Fig. 6 and was shown qualitatively in Fig. 5. At the onset of the jets, three shear layers are identified: the inner shear layer of the inner jet, a middle shear layer on the inside of the coflow jet, and the outer shear layer of the coflow jet. The middle and inner shear layers form the wake of the inner nozzle lip. The development of the shear layers is tracked by recording the "radial" location ($y_{0.5}/D_o$) of the point, which has a velocity equal to 50% of the maximum velocity difference across each shear region.

A defining factor in the downstream development of a jet is the initial condition at the exit. The shape and details of the initial mean velocity and the turbulence intensity profiles are of critical importance in interpreting the observed differences in the development of the axisymmetric and square coaxial nozzles. Note from Fig. 6 that the initial mean profiles ($x/D_o = 0$) of the axisymmetric and square (SS scan) nozzles are almost identical in the inner nozzle region and the wake created after the inner nozzle lip. The core of the inner jet is uniform and the fluctuation level low (fraction of a percent), with a small peak inside the inner shear layer near the inner jet wall. However, a considerable difference exists between the mean profiles in the core of the coflow region. The axisymmetric coflow jet core is considerably more uniform than its square counterpart, which has the shape of a simple shear flow, more so than the one from the circular jet. In both cases, the maximum velocity occurs closer to the inner wall. The difference between the axial fluctuation profiles in this region is more substantial. The maximum fluctuation level is observed near the middle of the coflow core for the square nozzle case with secondary peaks inside the two bounding shear layers, the middle shear layer near the inner wall of the outer jet, and the outer shear layer of the outer jet. No such peak is present in the core of the axisymmetric coflow, and the highest fluctuation levels are observed inside the bounding shear layers. Contrary to the square-jet side scan (SS), the shapes of the initial mean and fluctuation profiles along the square-jet diagonal scan (SDSD) are almost exactly similar to those of the axisymmetric jet, and the fluctuation levels are of the same magnitude. In the case of the square nozzle, the side-to-diagonal ratio of the outer shear-layer momentum thickness was approximately three. Thus, there is a significant azimuthal nonuniformity of the outer shear-layer thickness. Such a condition has been found to be detrimental to the development of axis switching[10] and may be a contributing reason to the absence of axis switching in our experiments.

On the basis of the measured profiles and with the aid of the time-averaged visualization, the coaxial jets can be divided into distinct regions, in a manner similar to that carried out by Ko and Au.[2] The first region is the one immediately downstream of the jet exit (approximately $0 < x/D_o < 0.5$), where the inner jet core decelerates. At the end of this region, the wake of the inner jet has completely disappeared as the inner and middle mixing layers merge, as evidenced in Fig. 6. In the second region (approximately $0.5 < x/D_o < 1.6$), the potential core of the inner jet persists at a fixed centerline velocity. At the end of this second region this potential core disappears, and the middle shear regions merge. This is evident in Fig. 6 from the time-averaged visualization and the velocity profiles at $x/D_o = 1.6$. The potential core of the inner jet disappears somewhat faster in the case of the square nozzle. The relative shapes of the coflow jet core profiles are preserved in these two regions, whereas the peak mean velocity remains more or less fixed. By the end of the second region, the original middle peak in fluctuation intensity has disappeared, and the highest fluctuation intensity is observed inside the outer coflow shear layer thereafter. In the same neighborhood, the averaged visualization (Fig. 6) indicates that outer and middle shear layers merge. This occurs earlier for the square nozzle across its sides (SS scans in Fig. 6a). The fluctuation level in the core of the square-jet coflow is initially considerably higher (by more than a factor of two) than that observed in the same region of the axisymmetric jet. The significant differences observed in the initial region profiles between the axisymmetric and square- (SS scan) jet coflows explain the higher mixing and inward spread of the outer

coflow shear layer qualitatively documented by the visualizations of Figs. 3 and 4. Such significantly enhanced growth was not observed along the diagonal of the square jet where the initial profile of the coflow mean velocity is more uniform, fluctuation level lower, and the profile shapes similar to the axisymmetric ones. The turbulence intensity along the centerline increases steadily within both initial regions described earlier, much like in a single jet.

The process of gradual merging of the opposite middle shear layers takes place within the third region of the coaxial jet (approximately $1.6 < x/D_o < 8$), as seen in Fig. 6. The centerline velocity minimum increases gradually until it becomes an absolute maximum at the end of the region. As the middle shear layers weaken, the corresponding maximum in turbulence intensity is eliminated until only one peak remains at the end of this region, corresponding to the outer shear layer. The centerline turbulence intensity reaches a peak in the beginning of this third region and gradually decays to a plateau at the end of the region (near $x/D_o = 8$, as seen in Fig. 6). Note from Fig. 6 that, after the middle shear-layer growth has completely overwhelmed the core of the inner jet (near $x/D_o = 2.4$), the axisymmetric and square- (SS scan) jet mean and fluctuation profiles become very nearly identical in magnitude and shape. The fourth region beyond $x/D_o = 8$ displays the characteristics of a "single jet" with a single centerline maximum of the mean velocity and a single off-center peak in turbulence intensity associated with the outer shear layer (see Fig. 6). In this region, the centerline turbulence intensity remains approximately constant as the centerline velocity begins to decay. Note that, on superposition, the square-jet diagonal profiles (SDSD scan) collapse onto those obtained from the SS scan and the axisymmetric nozzle case in the beginning of this fourth region. This indicates that the memory of the geometrical origin of the jet is being lost, or it could be construed as weak evidence of an "axis-switching" phenomenon in progress.

Figure 6 also indicates that the middle shear-layer development is nearly identical between the axisymmetric and square (SS scan) jets. This is in agreement with the mean and fluctuation profiles being nearly identical between the two jets within the middle shear layer. The middle shear layer on the diagonal of the square jet exhibits a much faster inward growth than that in the SS direction. The inward growth of the middle shear layers is slowed down considerably past the end of the second region, where the inner jet is completely overwhelmed and the mean shear is diminished. These discussed trends are quantified in Table 2, where the growth rates of the half-width ($dy_{0.5}/dx$) and the thickness ($d\delta/dx$) of the shear layers are listed. The middle shear layer for the axisymmetric nozzle and the SS direction of the square nozzle ceases to exist at around $x/D_o = 8$. However, it persists past that point on the diagonal, as is also insinuated by Fig. 3Sc. The growth of the outer shear layer is distinctly different between the axisymmetric and square nozzle in the SS direction. The initial location of the half-velocity point is also different as a consequence of the difference in the initial profiles. As observed qualitatively in the visualizations in the background of the profiles of Fig. 6 and quantitatively in Table 2, the near-field growth of the outer shear layer for the square nozzle in the SS direction is somewhat faster than that in the axisymmetric case. This can again be explained by virtue of the difference in the corresponding initial profiles. The growth of the outer shear layer on the diagonal is quite different. It is seen in Fig. 6b and Table 2 that, after a short period of no growth, a local contraction (negative growth) of the outer shear layer is documented, followed by a second region of growth. That the outer shear-layer half-width on the side (SS) increases, whereas it diminishes on the diagonal (SDSD), is a possible indication of a weak tendency toward axis switching near the exit of the nozzle. However, in the absence of strong visualization and quantitative evidence (crossover of the half-widths), one cannot conclude that this phenomenon actually takes place. This is not surprising given that it has been shown in single noncircular jets that axis switching is very sensitive to the initial conditions and the degree of large-scale structure coherence in the near field, which is very low in our case.

Scaled velocity and turbulence intensity profiles from the three shear regions of the coaxial flow are presented in Fig. 7. Scaling typically used in shear layers has been employed, following the example of Ko and Au.[2] The trends of their scaled data from axisymmetric

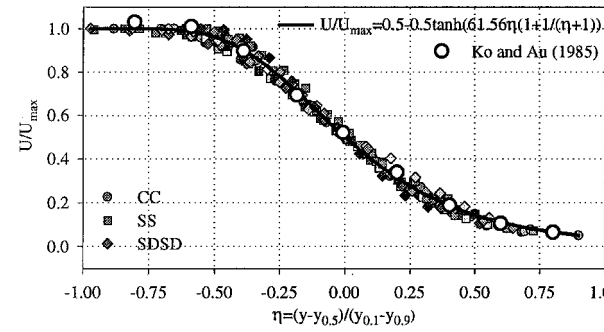

a) Outer shear layer mean velocity (x/D_o = 1.6, 2.4, 3.2, 6, 8)

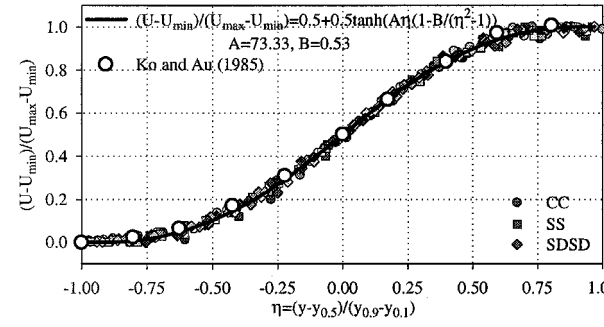

b) Middle shear layer mean velocity (x/D_o = 0, 0.13, 0.27, 0.53, 0.8, 1.6, 2.4, 3.2)

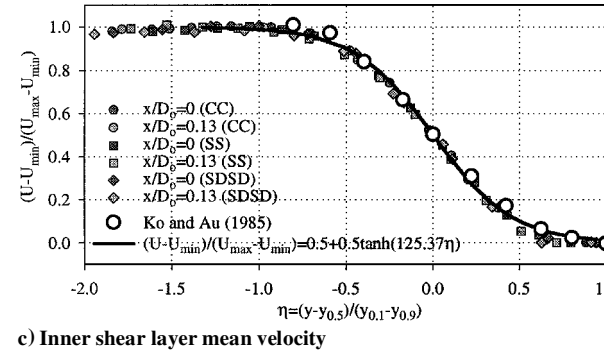

c) Inner shear layer mean velocity

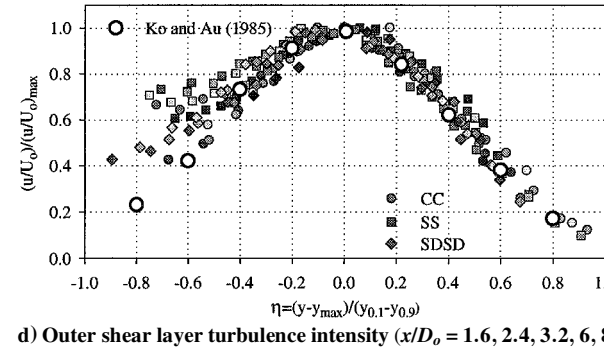

d) Outer shear layer turbulence intensity (x/D_o = 1.6, 2.4, 3.2, 6, 8)

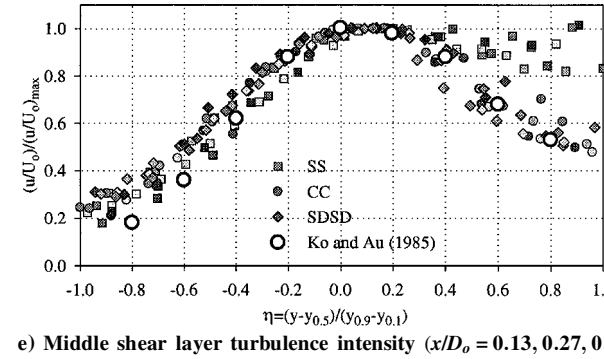

e) Middle shear layer turbulence intensity (x/D_o = 0.13, 0.27, 0.53, 0.8, 1.6)

Fig. 7 Scaled velocity and turbulence intensity profiles for square and circular coaxial nozzles: $Re_0 = 1.9 \times 10^4$ and $\lambda = 0.3$.

Table 2 Shear-layer growth rates

	Middle shear layer						Outer shear layer					
	$dy_{0.5}/dx(\times 10^3)$			$d\delta/dx(\times 10^2)$			$dy_{0.5}/dx(\times 10^3)$			$d\delta/dx(\times 10^2)$		
x/D_o	CC	SS	SDSD	CC	SS	SD	CC	SS	SD	CC	SS	SDSD
0.27	105	85	225	19	19	35	5	38	−98	3	35	2
0.53	105	100	155	22	20	33	0	56	−48	25	38	14
1.6	88	92	92	10	11	16	17	40	−12	18	18	19
2.4	37	31	34	4	5	5	33	48	8	16	12	17

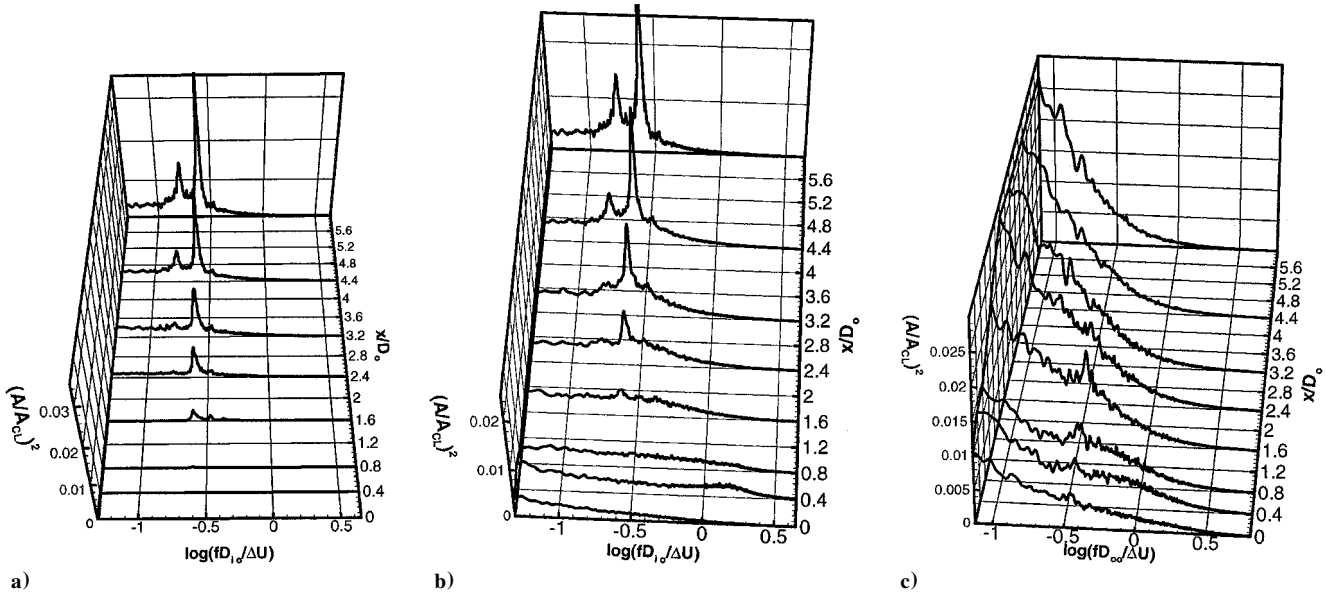

Fig. 8 Velocity spectra from a circular coaxial nozzle flow at $Re_0 = 1.9 \times 10^4$ and $\lambda = 0.3$: a) centerline, b) middle mixing region, and c) outer mixing region.

coaxial nozzles at various velocity ratios less than unity have been used for comparisons and to put the present data into perspective. Best fits of the scaled mean velocity profiles with typical hyperbolic tangent profiles are also included in Figs. 7a–7c. It is evident from Fig. 7 that the scaled mean profiles from both the axisymmetric and square (SS and SDSD scans) nozzle flows collapse on a single trend to a very satisfactory extent for all shear layers. This is more so for the middle and inner shear layers. The outer shear layer displays a higher degree of scatter. This is so primarily because the outer shear layer is less cleanly defined at the onset of the coflow jet flow as discussed earlier. The agreement with Ko and Au[2] is also very good. The scaling of the turbulence intensity is somewhat less clean. In the case of the outer layer, the scaling is good, whereas some deviations are observed, primarily for the SS scans of the square nozzles. It is speculated that this is the case for the same reason that causes the higher scatter in the mean scaled profiles. The agreement with Ko and Au[2] is reasonable considering that their turbulence profiles also displayed some scatter and that fewer downstream locations were included in their scaling. The turbulence intensity scaling is also good for the middle shear layer. In fact, it is very good to the left of the turbulence peak, whereas it breaks down for the SS scan of the square nozzle to the right of the peak for the same reason discussed earlier. The comparison to Ko and Au[2] is quite good considering the difference in coflow initial conditions between our study and theirs.

Velocity Spectra

Scaled velocity spectra obtained along the centerlines, as well as the inner and outer mixing regions, of both circular and square nozzles (SS section) are shown in Figs. 8 and 9, respectively. The spectra for each axial location from all mixing regions were taken at a transverse location corresponding to the point of maximum velocity fluctuation in the neighborhood of the corresponding shear-layer midpoint. The amplitude scaling is such that all spectral amplitudes are referred to the initial centerline point for each nozzle geometry. Thus, relative comparisons of spectral magnitude characteristics are possible between the two geometries examined. The frequencies are scaled to reflect the Strouhal number based on a relevant geometrical length scale and the velocity difference between the maximum and minimum across the corresponding shear region. Note that the centerline spectra at the exit of the jets have several peaks at frequencies that match the acoustic characteristics of the nozzle chamber. These peaks are not visible in Figs. 8a and 9a due to the nature of the scaling. In the immediate near field of the nozzles at $x/D_o = 0.4$ within the middle mixing region, a broad peak is observed in both the circular (Fig. 8b) and square (Fig. 9b) nozzle flows. At this downstream location, the inner core of the velocity profile is still flat, and the middle shear layer has its own identity, unlike further downstream where a wakelike profile develops as the inner uniform core disappears (see Fig. 6). Consequently, the observed local peak in the spectrum should be associated with the shear-layer preferred mode. Indeed, the observed frequency peaks at 1024 Hz for the circular nozzle and 1150 Hz for the square one correspond to the preferred modes of the corresponding shear layers. This is revealed by examining the associated Strouhal numbers. These were calculated using classical shear-layer scaling, based on the initial momentum thickness and the velocity jump magnitude, and they are in reasonably good agreement with linear stability estimates of the dominant shear-layer mode Strouhal numbers calculated by a linear stability code previously used by Nikitopoulos and Liu[22,23] and Nikitopoulos and Seo.[24] Downstream of the exit, prominent frequency peaks appear in the centerline (Figs. 8a and 9a) and middle mixing region (Figs. 8b and 9b) spectral records of both the circular and square nozzle flows. The individual peaks correspond to initial peaks at the exit and are both within a range in the neighborhood of the most amplified frequency for the wakelike profile that develops in the midfield of the inner mixing region based on linear stability. The frequencies with the peak amplitudes are virtually identical for the circular (111- and 166-Hz) and square (115- and 169-Hz)

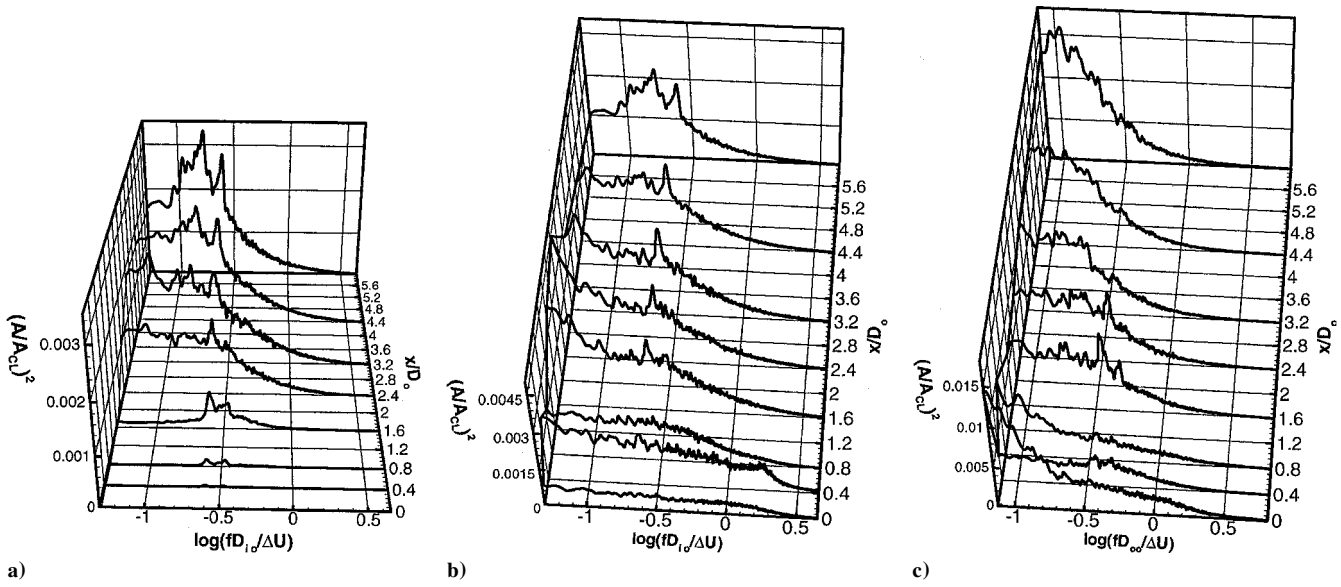

Fig. 9 Velocity spectra from a square coaxial nozzle flow at $Re_0 = 1.9 \times 10^4$ and $\lambda = 0.3$: a) centerline, b) middle mixing region (SS), and c) outer mixing region (SS).

configurations. They are amplified throughout the evolution of the inner region in the near and midfield, as are the less prominent frequencies in that neighborhood of the spectrum. This is not unusual because the frequency-amplification rate curve, as predicted by linear stability, is relatively flat in the neighborhood of the most amplified frequency, allowing amplification of a band of frequencies around the preferred mode. The main differences in the spectra of the inner region midfield between the circular and square nozzle flows are in the breadth and magnitude of the peak frequencies as they evolve downstream. The spectral peaks are sharper and stronger in the case of the circular nozzles compared to the broader and weaker ones of the square nozzles. In both geometries, the higher of the two observed discrete frequencies becomes dominant in the near field of the inner region, whereas the lower one, which is approximately $\frac{2}{3}$ of the higher, emerges. In the midfield of the inner region, the higher frequency remains dominant in the case of the circular geometry, whereas it assumes a secondary role in the case of the square geometry. In the latter case, the lower discrete frequency becomes dominant in the midfield, although its peak is much broader than its counterpart of the circular nozzle.

The shear layer of the outer mixing region is initially highly turbulent at the exit, more so than the one in the middle mixing region. Therefore, the initial spectra at the exit are broadband and were found to display a $-\frac{5}{3}$ inertial range when plotted on a log–log scale. The discrete peaks observed in the near field of the outer shear layers of both circular (Fig. 8c) and square (Fig. 9c) configurations are at 166 Hz. By the application of shear-layer scaling, it was determined that this frequency is too low to be related to the outer shear-layer preferred mode. It is apparent that its appearance is a reflection of the development of the wake mode of the middle mixing region in the beginning of the coaxial jet midfield. This notion is reinforced by this discrete frequency peak occuring in the neighborhood where the outer mixing layer meets the inner mixing region at the end of the coflow unmixed core, as observed in Fig. 4. As the already turbulent outer shear layer grows and develops further downstream, all spectral peaks disappear, and the $-\frac{5}{3}$ inertial range is fully reestablished. Note that no local peak is observed at a frequency corresponding to the preferred mode of the outer shear layer. This is justified by this shear layer being initially highly turbulent and the flow being unforced, other than the acoustic modes of the nozzle interior, which are weak compared to the broadband turbulent spectrum strength in the outer shear layer and not tuned to the outer shear-layer mode.

Similar trends to those described for the SS section of the square nozzle are observed when examining the spectral evolution in the middle and outer mixing regions of the SDSD (diagonal) section. The spectral evolution on the diagonal plane is shown in Fig. 10. The

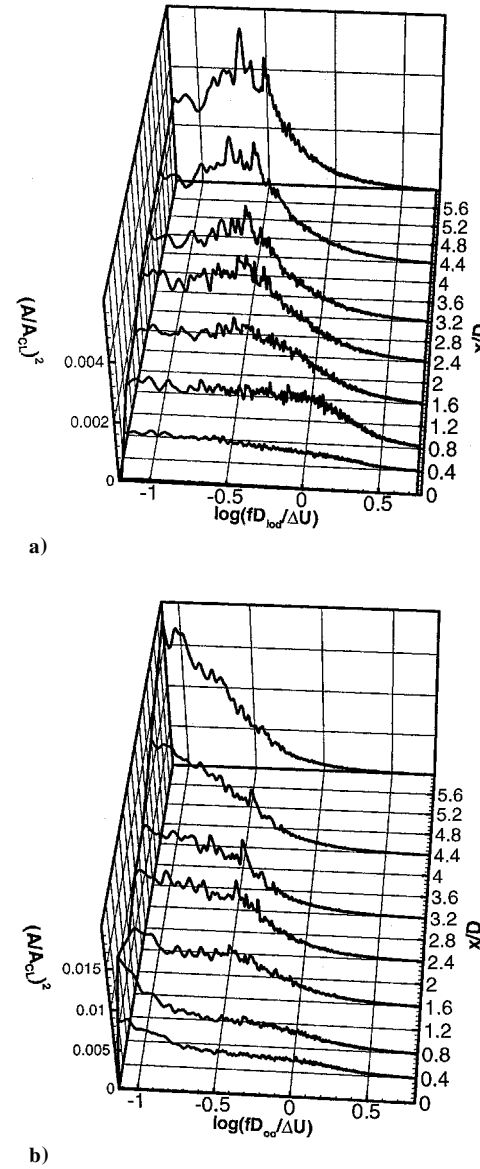

Fig. 10 Velocity spectra from a square coaxial nozzle flow at $Re_0 = 1.9 \times 10^4$ and $\lambda = 0.3$: a) middle mixing region (SDSD) and b) outer mixing region (SDSD).

middle mixing region of Fig. 10a displays two broad, yet discrete, peaks (115 and 169 Hz) in the same fashion as in the center plane according to Fig. 9b. The initial emergence of the higher frequency in the beginning of the jet midfield and the shift toward the lower frequency further downstream are consistent with the centerline and center plane behaviors. Unlike the case of the square nozzle center plane, a distinct preferred mode associated with the middle shear layer is not observed along the diagonal. Instead, a rapid "filling" of the spectrum appears in the range of frequencies commensurate with the expected preferred mode based on a Strouhal number calculated from free mixing layer scaling. The absence of a discrete preferred mode can be attributed to the more vigorous production of smaller scales due to the corner flows on the diagonal. The outer shear-layer spectra shown in Fig. 10b also reveal the same features observed before on the center plane. The initial shear layer is highly turbulent and the frequency peak, which appears in the midfield at a distance from the exit corresponding to the merging of the outer and middle mixing regions, is a reflection of the middle mixing region wake mode. No local spectral peak associated with the shear layer is observed on this plane either. A $-\frac{5}{3}$ inertial range is observed from the onset of the outer shear layer at the outer nozzle exit and is maintained throughout its evolution.

Conclusions

A qualitative and quantitative investigation of unforced, initially turbulent flows emanating from equivalent geometries of axisymmetric (circular) and square coaxial nozzles has been carried out. Flow visualization and velocity measurements were performed at a coflow jet Reynolds number of 1.9×10^4 and at an inner-to-outer jet velocity ratio of 0.3. Scaling of mean velocity and turbulence profiles for the three shear layers formed in the near field of axisymmetric and square coaxial flows was found to be consistent between the two geometries and with previously reported trends for axisymmetric coaxial jets.

Large-scale periodic structures were identified for both nozzle configurations in the midfield of the inner mixing region, which has wake characteristics. The frequency of the observed spectral peaks in this region scaled using wake scales correspond to Strouhal number values consistent with those expected for a wake on the basis of linear stability. The outer mixing region, which is highly turbulent, displays a $-\frac{5}{3}$ inertial range from its onset at the nozzle exit and shows no signs of an indigenous coherent organized structure. The spectra obtained in the square nozzle mixing regions both on the center plane and the diagonal planes are mutually consistent, indicating the same broad frequency peaks. The spectra from the turbulent shear layers of the middle mixing region near field indicate the presence of a short-lived shear-layer preferred mode at a much higher frequency than the one associated with the subsequent development of the wake downstream. The spectral characteristics of the circular and square nozzle combinations are qualitatively similar. However, the discrete frequency peaks associated with the wake of the inner mixing region are much broader in the case of the square nozzles, and the dominant frequency at the end of the midfield within the inner mixing region is lower than that of the circular ones. This is explained by the higher overall turbulence intensity in the inner mixing region of the square nozzles.

The existence of axis switching, a phenomenon observed in single nonaxisymmetric nozzles, is not evident from visualizations and measurements in the square coaxial nozzle. The lack of axis switching is attributed to the initial low coherence of large-scale structures (azimuthal vorticity) in the shear layers, the initially high small-scale turbulence levels in the outer flow, and strong azimuthal nonuniformity of the outer shear layers. These factors have been identified in past studies[5,10] of single noncircular jets as factors detrimental to axis switching. Thus, it is not surprising that this phenomenon did not occur. In spite of the absence of axis switching, visualizations and local velocity measurements have indicated modest mixing enhancement on the side plane in the square nozzles compared to the circular ones. This can be largely attributed to local differences in the initial velocity profiles between these two configurations and, particularly, to the higher initial turbulence intensity levels in the outer flow on the side of the square nozzle. The potential for development of axis switching in coaxial noncircular nozzle flows needs further investigation. Thus, additional work is necessary to determine to what extent mixing enhancement, other than the geometrical increase of the area subjected to shear or that caused by differences in initial conditions, can be produced using square coaxial nozzles as opposed to axisymmetric ones. Nozzles with initial conditions more favorable to axis switching and/or application of active forcing could answer this question and reveal if this phenomenon is at all possible in noncircular coaxial nozzle flows.

Acknowledgments

This work has been supported by NASA, the Louisiana Board of Regents Louisiana Education Quality Support Fund, and the U.S. Air Force Office of Scientific Research Graduate Student Research Program. The guidance and help of W. M. Roquemore of the U.S. Air Force Research Laboratory and helpful discussions with E. J. Gutmark while at Louisiana State University are also gratefully acknowledged.

References

[1]Ko, N. W. M., and Kwan, A. S. H., "The Initial Region of Subsonic Coaxial Jets," *Journal of Fluid Mechanics*, Vol. 73, 1976, pp. 305–332.

[2]Ko, N. W. M., and Au, H., "Coaxial Jets of Different Mean Velocity Ratios," *Journal of Sound and Vibration*, Vol. 100, No. 2, 1985, pp. 211, 212.

[3]Dahm, W. J. A., Frieler, C. E., and Tryggvason, G., "Vortex Structure and Dynamics in the Near Field of a Coaxial Jet," *Journal of Fluid Mechanics*, Vol. 241, 1992, pp. 371–402.

[4]Tang, D. K., and Ko, N. W. M., "Coherent Structure Interactions in Excited Coaxial Jet of Mean Velocity Ratio of 0.3," *AIAA Journal*, Vol. 31, No. 8, 1993, pp. 1521–1524.

[5]Zaman, K. B. M. Q., "Axis Switching and Spreading of an Asymmetric Jet: The Role of Coherent Structure Dynamics," *Journal of Fluid Mechanics*, Vol. 316, 1996, pp. 1–27.

[6]Sforza, P. M., Steiger, M. H., and Trentacoste, N., "Studies on Three-Dimensional Viscous Jets," *AIAA Journal*, Vol. 4, No. 5, 1966, pp. 800–806.

[7]Trentacoste, N., and Sforza, P., "Further Experimental Results for Three-Dimensional Free Jets," *AIAA Journal*, Vol. 5, No. 5, 1967, pp. 885–891.

[8]duPlessis, M. P., Wang, R. L., and Kahawita, R., "Investigation of the Near-Region of a Square Jet," *Journal of Fluids Engineering*, Vol. 96, Sept. 1974, pp. 247–251.

[9]Quinn, W. R., and Militzer, J., "Experimental and Numerical Study of a Turbulent Free Square Jet," *Physics of Fluids*, Vol. 31, No. 5, 1988, pp. 1017–1025.

[10]Grinstein, F. F., Gutmark, E., and Parr, T., "Near Field Dynamics of Subsonic Free Square Jets. A Computational and Experimental Study," *Physics of Fluids*, Vol. 7, No. 6, 1995, pp. 1483–1497.

[11]Quinn, W. R., "Streamwise Evolution of a Square Jet Cross Section," *AIAA Journal*, Vol. 30, No. 12, 1992, pp. 2852–2857.

[12]Schadow, K. C., Gutmark, E., Parr, D. M., and Wilson, K. J., "Selective Control of Flow Coherence in Triangular Jets," *Experiments in Fluids*, Vol. 6, 1988, pp. 129–135.

[13]Koshigoe, S., Gutmark, E., Schadow, K. C., and Tubis, A., "Wave Structures in Jets of Arbitrary Shape. III. Triangular Jets," *Physics of Fluids*, Vol. 31, No. 6, 1988, pp. 1410–1419.

[14]Schadow, K. C., Gutmark, E., Wilson, K. J., and Smith, R. A., "Noncircular Inlet Duct Cross-Section to Reduce Combustion Instabilities," *Combustion Science and Technology*, Vol. 73, 1990, pp. 537–553.

[15]Ho, C.-M., and Gutmark, E., "Vortex Induction and Mass Entrainment in a Small-Aspect-Ratio Elliptic Jet," *Journal of Fluid Mechanics*, Vol. 179, 1987, pp. 383–405.

[16]Hussain, F., and Husain, H. S., "Elliptic Jets. Part 1. Characteristics of Unexcited and Excited Jets," *Journal of Fluid Mechanics*, Vol. 208, 1989, pp. 257–320.

[17]Husain, H. S., and Hussain, F., "Elliptic Jets. Part 2. Dynamics of Coherent Structures: Pairing," *Journal of Fluid Mechanics*, Vol. 233, 1991, pp. 439–482.

[18]Husain, H. S., and Hussain, F., "Elliptic Jets. Part 3. Dynamics of Preferred Mode Coherent Structure," *Journal of Fluid Mechanics*, Vol. 248, 1993, pp. 315–361.

[19]Gutmark, E., and Ho, C.-M., "Visualization of a Forced Elliptic Jet," *AIAA Journal*, Vol. 24, No. 4, 1986, pp. 684, 685.

[20]Bitting, J. W., Nikitopoulos, D. E., Gogineni, S. P., and Gutmark, E. J., "Visualization of Non-Circular, Coaxial Nozzle Flow Structure," *Bulletin of the American Physical Society*, Vol. 42, No. 11, 1997, p. 2115.

[21]Bitting, J. W., Nikitopoulos, D. E., Gogineni, S. P., and Gutmark, E. J., "Structure of Square Coaxial Nozzle Flows," AIAA Paper 98-2917, June 1998.

[22]Nikitopoulos, D. E., and Liu, J. T. C., "Nonlinear Binary-Mode Interactions in a Developing Mixing Layer," *Journal of Fluid Mechanics*, Vol. 179, 1987, pp. 345–370.

[23]Nikitopoulos, D. E., and Liu, J. T. C., "Nonlinear Three-Wave Interactions in a Developing Mixing Layer," *Physics of Fluids*, Vol. 13, No. 4, 2001, pp. 966–982.

[24]Nikitopoulos, D. E., and Seo, T., "Two- and Three-Dimensional, Large-Scale Mode Interactions in a Developing Shear Layer," *Bulletin of the American Physical Society*, Vol. 42, No. 11, 1997, p. 2192.

W. J. Devenport
Associate Editor